Equilibria, kinetics, and boron isotope partitioning in the aqueous boric acid – hydrofluoric acid system

Richard E. Zeebe*,[1] and James W. B. Rae[2]

*Corresponding Author.

[1]School of Ocean and Earth Science and Technology, Department of Oceanography, University of Hawaii at Manoa, 1000 Pope Road, MSB 629, Honolulu, HI 96822, USA.

zeebe@soest.hawaii.edu

[2]School of Earth & Environmental Sciences, The Irvine Building, St. Andrews, KY16 9AL, UK. jwbr@st-andrews.ac.uk

Revised Version.

To be resubmitted to *Chemical Geology*.

May 18, 2020

Abstract. The aqueous boric, hydrofluoric, and fluoroboric acid systems are key to a variety of applications, including boron measurements in marine carbonates for CO_2 system reconstructions, chemical analysis and synthesis, polymer science, sandstone acidizing, and more. Here we present a comprehensive study of chemical equilibria and boron isotope partitioning in the aqueous boric acid – hydrofluoric acid system. We work out the chemical speciation of the various dissolved compounds over a wide range of pH, total fluorine (F_T), and total boron (B_T) concentrations. We show that at low pH ($0 \leq p\text{H} \leq 4$) and $F_T \gg B_T$, the dominant aqueous species is BF_4^-, a result relevant to recent advances in high precision measurements of boron concentration and isotopic composition. Using experimental data on kinetic rate constants, we provide estimates for the equilibration time of the slowest reaction in the system as a function of pH and [HF], assuming $F_T \gg B_T$. Furthermore, we present the first quantum-chemical (QC) computations to determine boron isotope fractionation in the fluoroboric acid system. Our calculations suggest that the equilibrium boron isotope fractionation between BF_3 and BF_4^- is slightly smaller than that calculated between $B(OH)_3$ and $B(OH)_4^-$. Based on the QC methods X3LYP/6-311+G(d,p) (X3LYP+) and MP2/aug-cc-pVTZ (MP2TZ), $\alpha_{(BF_3-BF_4^-)} \simeq 1.030$ and 1.025, respectively. However, BF_4^- is enriched in ^{11}B relative to $B(OH)_4^-$, i.e., $\alpha_{(BF_4^- - B(OH)_4^-)} \simeq 1.010$ (X3LYP+) and 1.020 (MP2TZ), respectively. Selection of the QC method (level of theory and basis set) represents the largest uncertainty in the calculations. The effect of hydration on the calculated boron isotope fractionation turned out to be minor in most cases, except for BF_4^- and $B(OH)_3$. Finally, we provide suggestions on best practice for boric acid – hydrofluoric acid applications in geochemical boron analyses.

1 Introduction

Fluroboron compounds have a wide variety of uses. A recent geochemical application is in the high precision analysis of boron concentration and isotopic composition (Misra et al., 2014b; Rae et al., 2018; He et al., 2019). These boron measurements have application in marine carbonates as tracers of the CO_2 system (e.g., Branson, 2018; Rae, 2018; Hönisch et al., 2019), in silicates as tracers of seawater exchange with oceanic crust (Marschall, 2018) and subduction (De Hoog and Savov, 2018), and various other fundamental and environmental uses (e.g., Rosner et al., 2011; Penman et al., 2013; Guinoiseau et al., 2018). Boron trifluoride (BF_3) and fluoroboric acid (HBF_4) also have a wide range of applications in chemical analysis and synthesis. BF_3 is used in various organic synthesis reactions, such as the reduction of aldehydes and ketones to alcohols and hydrocarbons (Fry et al., 1978), due to its properties as a Lewis acid. HBF_4 is also used as a catalyst in organic synthesis and in the electroplating of tin and tin alloys, alongside various applications in polymer science, sandstone acidizing, manufacturing of fluoroborate salts, and more (e.g., Palaniappan and Devi, 2008; Leong and Ben Mahmud, 2019).

CITE ABOVE? (Wei et al., 2013; Li et al., 2019)

While the chemical and isotopic equilibrium in the boric acid system in aqueous solution is relatively well understood, including $\alpha_{(B(OH)_3-B(OH)_4^-)}$(e.g. Zeebe, 2005; Liu and Tossell, 2005; Klochko et al., 2006; Nir et al., 2015), the partitioning of boron and its isotopes in the aqueous boric acid – hydrofluoric acid system has not been investigated in detail. This leads to uncertainties on how best to apply this method in laboratory procedures and potential pitfalls associated with isotope fractionation between B-F species. Here we work out the equilibria and kinetics of boron species in the presence of hydrofluoric acid, provide the first

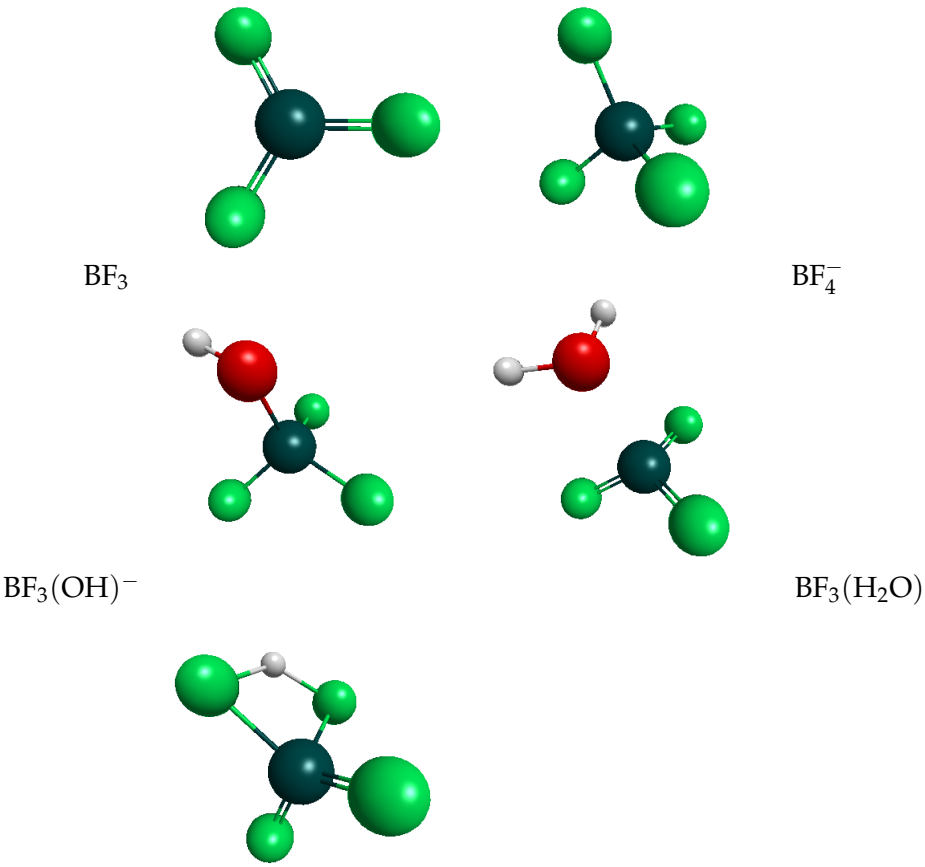

Figure 1. Geometries of several key compounds examined in this study. Structures shown were optimized using quantum-chemical calculations for isolated ("gas-phase") molecules. Dark-green: boron, light-green: fluorine, red: oxygen, white: hydrogen. The notations $BF_3(H_2O)$ and $HBF_3(OH)$ will be used synonymously here for structures similar to the $BF_3(H_2O)$ geometry shown (for details, see Section 4.1). (**I**) indicates geometrically unstable (one calculated frequency is imaginary).

quantum-chemical calculations for isotopic fractionation factors in this system, and comment on best practice in the practical application of HF in boron analyses.

2 Chemical Equilibrium

The reactions that link the boric acid – hydrofluoric acid system (involving B-F compounds, see Fig. 1) may be written as (Wamser, 1951; Mesmer et al., 1973):

$$B(OH)_3 + F^- \rightleftharpoons BF(OH)_3^- \quad (1)$$

$$B(OH)_3 + 2F^- + H^+ \rightleftharpoons BF_2(OH)_2^- + H_2O \quad (2)$$

$$B(OH)_3 + 3F^- + 2H^+ \rightleftharpoons BF_3(OH)^- + 2H_2O \quad (3)$$

$$B(OH)_3 + 4F^- + 3H^+ \rightleftharpoons BF_4^- + 3H_2O\,, \tag{4}$$

with

$$K_1 = \frac{[BF(OH)_3^-]}{[B(OH)_3][F^-]} \quad ; \quad K_2 = \frac{[BF_2(OH)_2^-]}{[B(OH)_3][F^-]^2[H^+]} \tag{5}$$

$$K_3 = \frac{[BF_3(OH)^-]}{[B(OH)_3][F^-]^3[H^+]^2} \quad ; \quad K_4 = \frac{[BF_4^-]}{[B(OH)_3][F^-]^4[H^+]^3}\,. \tag{6}$$

In addition, we take into account the relatively well known dissociation reactions:

$$B(OH)_3 + H_2O \rightleftharpoons B(OH)_4^- + H^+ \tag{7}$$

$$HF \rightleftharpoons F^- + H^+ \tag{8}$$

$$H_2O \rightleftharpoons H^+ + OH^-\,, \tag{9}$$

with

$$K_B = \frac{[B(OH)_4^-][H^+]}{[B(OH)_3]}\,;\; K_F = \frac{[F^-][H^+]}{[HF]}\,;\; K_w = [H^+][OH^-]\,. \tag{10}$$

Furthermore, equilibrium between the four $BF_i(OH)_{4-i}^-$ ions ($i = 1, \ldots, 4$) in reactions (1)-(4) and their protonated forms $HBF(OH)_3$, $HBF_2(OH)_2$, $HBF_3(OH)$, and HBF_4 need to be considered. For example,

$$HBF(OH)_3 \rightleftharpoons BF(OH)_3^- + H^+ \quad ; \quad K_1' = \frac{[BF(OH)_3^-][H^+]}{[HBF(OH)_3]}\,, \tag{11}$$

and so forth.

Given the immediate reaction of BF_3 with water, gaseous BF_3 can likely be neglected for dilute solutions at room temperature. For example, complete absorption of 1.17 mol BF_3 per kg H_2O has been reported at 25°C with no BF_3 observed by infrared analysis in the vapor phase (Scarpiello and Cooper, 1964). Some gas manufacturers state BF_3 "solubilities" of ~3.2 g per g H_2O at 0°C (47 mol BF_3/kg H_2O), yet the origin and method for obtaining this value is

difficult to track down. Also, "solubility" appears misleading here as hydrates are instantly formed, rather than dissolved BF_3. Raman spectra of a BF_3-H_2O mix (ratio 1:2) showed three of the four fundamentals of a tetrahedral molecule (not of a trigonal molecule like BF_3), almost identical to those of an aqueous $NaBF_3(OH)$ solution (Maya, 1977). These observations are consistent with Anbar and Guttmann (1960)'s estimate of $[HBF_3(OH)]/[BF_3] \simeq 5\times10^6$ based on free energies.

The equilibrium constants K_i have been determined in 1 M $NaNO_3$ and 1 M NaCl solutions (Grassino and Hume, 1971; Mesmer et al., 1973); K_B, K_F, and K_w are relatively well known, also at different ionic strengths. In this study, we use the set of constants given by Mesmer et al. (1973) in 1 M NaCl (see Table 1). The acid dissociation constants K_i' are less well known. For instance, the acid strength of HBF_4 has been estimated to be similar to HCl and H_2SO_4 in aqueous solution (Wamser, 1951; Fărcasiu and Hâncu, 1997). Thus, we assign the value $pK_4' = -3.0$ (actual value is of minor importance as long as $\lesssim -2.0$). The acid strength of $HBF_3(OH)$ and $HBF_2(OH)_2$ was deemed similar to CCl_3COOH and $CHCl_2COOH$, respectively (Wamser, 1951), broadly consistent with estimates based on $HBF_3(OH)$ and $HBF_2(OH)_2$ concentrations in solution (Mesmer et al., 1973). Hence we use $pK_3' = 0.66$ and $pK_2' = 1.35$ (Lide, 2004). For the weakest of the four acids, $HBF(OH)_3$, we assign $pK_1' = 2.0$ (actual value is of minor importance as long as $\lesssim 5.0$) (Table 1).

To link equilibrium and kinetics, the equilibrium constant for the hydrolysis of fluoboric acid will also be required (see reaction (13), Section 3 below):

$$K_h = \frac{[BF_3(OH)^-][HF]}{[BF_4^-]}\,, \tag{12}$$

which we set to $K_h = 2.3\times10^{-3}$ M ($pK_h = 2.64$, Wamser, 1948) at 25°C for consistency with Wamser's kinetic data used in Section 3. Compatibility between K_h and the set of K's from

Table 1. Equilibrium constants at 25°C used in this study ($p\mathrm{K} = -\log K$).

pK	pK_1	pK_2	pK_3	pK_4	pK_B	pK_F	pK_w	pK'_1	pK'_2	pK'_3	pK'_4	pK_h
Note	*a*	*a*	*a*	*b*	*a*	*a*	*a*	*b*	*b*	*b*	*b*	*c*
Value	0.36	−7.06	−13.69	−19.21	8.81	2.89	13.73	2.00	1.35	0.66	−3.00	2.64

[a] Mesmer et al. (1973), 1 M NaCl.

[b] See text.

[c] Wamser (1948).

Mesmer et al. (1973) (Table 1), then determines $pK_4 = -19.21$, because $K_4 = K_3/K_F/K_h$. Note that Mesmer et al. (1973) did not measure K_4 but determined its value using the same reasoning as applied here.

Given equilibrium constants, pH, total boron and total fluorine, the speciation in the boric acid – hydrofluoric acid system can be calculated (Appendix A). At low pH ($0 \leq p\mathrm{H} \leq 4$) and $\mathrm{F}_T \gg \mathrm{B}_T$, the dominant aqueous species is BF_4^-, followed by $\mathrm{BF}_3(\mathrm{OH})^-$ (Fig. 2). Also, under most of those conditions, the protonated forms $[\mathrm{HBF}_i(\mathrm{OH})_{4-i}]$ make up a small fraction of B_T and F_T (not shown). One exception is $\mathrm{HBF}_3(\mathrm{OH})$ with significant concentrations at very low pH (Fig. 2). However, note that there is considerable uncertainty in the calculated $[\mathrm{HBF}_3(\mathrm{OH})]$, as only estimated values for pK'_3 are available (see above). Our speciation results (Fig. 2) are similar to, but different from, those of Katagiri et al. (2006), who used a different set of constants and did not take into account the protonated forms $[\mathrm{HBF}_i(\mathrm{OH})_{4-i}]$.

The rising concentration of $\mathrm{HBF}_3(\mathrm{OH})$ at $[\mathrm{H}^+] > 10^0$ (negative pH) can be understood considering the relevant equilibria and their pK values (Table 1). At very high $[\mathrm{H}^+]$, the most abundant species are BF_4^-, $\mathrm{BF}_3(\mathrm{OH})^-$, HBF_4, and $\mathrm{HBF}_3(\mathrm{OH})$. As one might expect, at low pH, $[\mathrm{BF}_4^-] > [\mathrm{BF}_3(\mathrm{OH})^-]$. However, the balance between these species is additionally controlled

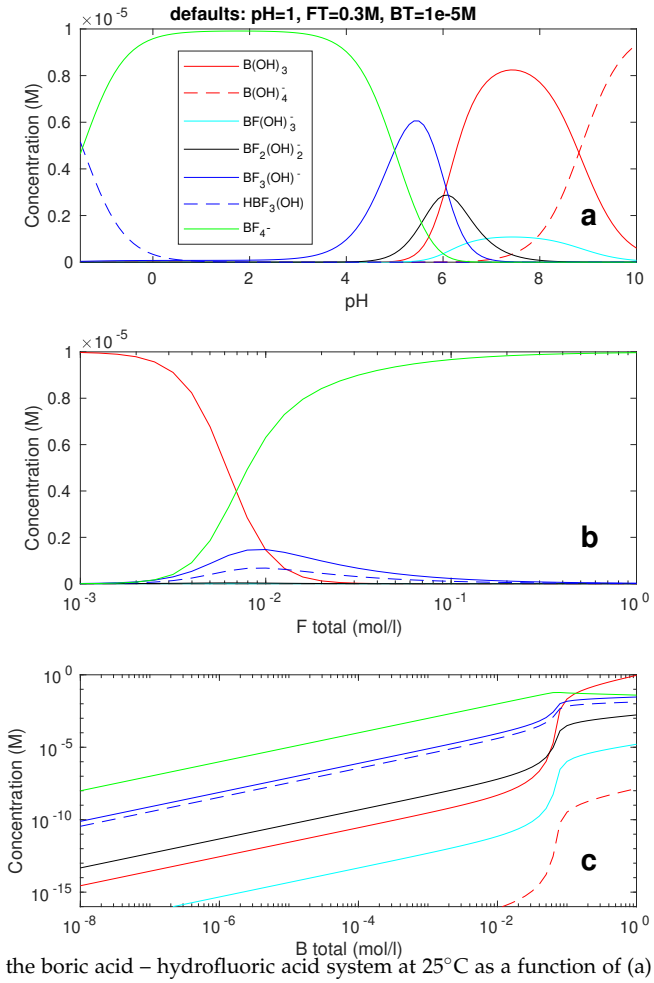

Figure 2. Speciation in the boric acid – hydrofluoric acid system at 25°C as a function of (a) pH, (b) F_T, and (c) B_T. Default parameter values (when not varied) are $p\mathrm{H} = 1.0$, $F_T = 0.3$ M, and $B_T = 1\times10^{-5}$ M. Note that $[HBF_3(OH)]$ is uncertain as only estimated values for pK_3' are available.

by the acid strengths of the protonated forms, HBF_4 and $HBF_3(OH)$, of which HBF_4 is the stronger acid (pK's of -3.00 vs. +0.66, see Table 1). It turns out that for the pK set used here, the difference in acid strength between HBF_4 and $HBF_3(OH)$ dominates that between BF_4^- and $BF_3(OH)^-$, leading to high $[HBF_3(OH)]$ at very low pH. In fact, using equilibrium relations such as Eqs. (6), (10), and (11), and $F_T \gg B_T$, the hydrogen ion concentration $[H^+]^*$ at which $[HBF_3(OH)] = [BF_4^-]$ can be estimated as $[H^+]^* \simeq K_3' K_4 K_F F_T / K_3$, or $p\mathrm{H}^* \simeq -1.5$, in agreement with the complete speciation calculation (Fig. 2).

2.1 Note of caution

For the present study, we opted for the set of equilibrium constants (K's) from Mesmer et al. (1973) (Table 1), as the set appears internally consistent. However, these K's apply to 1 M NaCl solutions and not to solutions of different ionic strengths in general. Unfortunately, the dependence on ionic strength is unknown at present. Mesmer et al. (1973) noted that their equilibrium constant for the hydrolysis of $BF_3(OH)^-$ to produce $BF_2(OH)_2^-$ and undissociated HF (1.8×10^{-4}) is considerably lower than the value 0.011 estimated by Wamser (1951). Furthermore, the acid dissociation constants K_i' have only been estimated, not measured, at this point. As a result, our equilibrium calculations (Fig. 2) should be taken as a basic guide to the speciation in the system. However, that speciation only applies to a single ionic strength and may also change in the future as new or improved data for equilibrium constants become available. Caution seems also warranted regarding the available kinetic data for the system, as values reported by two different studies for one particular rate constant differ by a factor of ~2-3 (see Section 3).

3 Kinetics

Among the reactions in the fluoroboric acid system, only the following is considered slow (Wamser, 1948, 1951; Anbar and Guttmann, 1960):

$$BF_3(OH)^- + HF \underset{k_2}{\overset{k_1}{\rightleftharpoons}} BF_4^- + H_2O\,, \tag{13}$$

which will be assumed the slowest reaction in the system and examined in the following. Reaction (13) leads to the rate law:

$$\frac{d[BF_4^-]}{dt} = k_1[BF_3(OH)^-][HF] - k_2[BF_4^-]\,. \tag{14}$$

Wamser (1951) found the forward reaction ((13) left to right) to be acid-catalyzed, with:

$$k_1 \;=\; k_1^0 + k_1^{\mathrm{H}}[\mathrm{H}^+]\,, \tag{15}$$

where $k_1^0 = 0.064\ \mathrm{l\,mol^{-1}\ min^{-1}}$ and $k_1^{\mathrm{H}} = 7.35$ at 25°C. The measured values in Table II of Wamser (1951) at $p\mathrm{H} = 1.65$ and 1.36 (0.244 and $0.387\ \mathrm{l\,mol^{-1}\ min^{-1}}$) are consistent with those in Table IV of Wamser (1948) (0.244 and $0.392\ \mathrm{l\,mol^{-1}\ min^{-1}}$) at 25°C. We are unaware of any other studies that determined k_1 experimentally.

Wamser (1948) also studied the $\mathrm{BF_4^-}$ hydrolysis, i.e., the backward reaction of (13) and provided values for k_2 (his Table IV), which varied with the initial concentration of $\mathrm{BF_4^-}$. Wamser (1948) stated that the observed variation of k_2 may be in part a result of $[\mathrm{H}^+]$ changes, which varied simultaneously with initial concentrations. In fact, Anbar and Guttmann (1960) found the $\mathrm{BF_4^-}$ hydrolysis to be first order in $[\mathrm{BF_4^-}]$ and $[\mathrm{H}^+]$ and suggested the rate law $R = k_2'[\mathrm{H}^+][\mathrm{BF_4^-}]$. Assuming also the $\mathrm{BF_4^-}$ hydrolysis to be acid-catalyzed and assuming $p\mathrm{H}$ values of 1.65 and 1.36 for initial concentrations of 0.0561 M and 0.1105 M in Table IV of Wamser (1948) (cf. Table II, Wamser (1951)), we can calculate a catalyzed hydrolysis rate constant from:

$$k_2 \;=\; k_2^0 + k_2^{\mathrm{H}}[\mathrm{H}^+]\,, \tag{16}$$

by fitting Eq. (16) to Wamser's k_2 values, which yields $k_2^0 = 1.47\times10^{-4}\ \mathrm{min^{-1}}$ and $k_2^{\mathrm{H}} = 1.69\times10^{-2}\ \mathrm{l\,mol^{-1}\ min^{-1}}$. The latter may be compared to $k_2' \simeq 7\times10^{-3}\ \mathrm{l\,mol^{-1}\ min^{-1}}$ given by Anbar and Guttmann (1960), which is less than half the k_2^{H} value as derived from Wamser (1948). The reason for the discrepancy is unclear at this point. However, note that the ratio of Wamser's $k_2/k_1 \simeq 2.3\times10^{-3}$ M (Table IV, Wamser (1948)), i.e., the equilibrium constant (K_h) of reaction (13), was consistent with his value derived from

titration data ($K_h = 2.04\times10^{-3}$ M). This lends confidence to the kinetic data of Wamser (1948, 1951), which we use in the following. Also, for internal consistency between k_1 and k_2 as implemented here (Eqs. (15) and (16)), we made sure that the ratios of individual k_i^j's that are dominant at low vs. high pH, respectively, yield the desired K_h value, i.e., $k_2^0/k_1^0 = 1.47\times10^{-4}/0.064 = k_2^{\mathrm{H}}/k_1^{\mathrm{H}} = 1.69\times10^{-2}/7.35 = 2.3\times10^{-3}$.

Given k_1 and k_2, the rate law (Eq. (14)) can be solved analytically with some critical assumptions (Appendix B). First, our solution is only valid at low pH, where $[BF_3(OH)^-]$ and $[BF_4^-]$ are the dominant B-F species and other compounds such as $BF_2(OH)_2^-$ and $BF(OH)_3^-$ can be ignored. Second, $[H^+]$ and $[HF]$ are assumed to remain constant during the reaction. If $[H^+]$ varies, our acid-catalyzed rates cannot be treated using constant k_1 and k_2 (Eqs. (15) and (16)). Importantly, constant $[HF]$ during the reaction usually requires the hydrofluoric acid concentration to be much greater than the total boron concentration B_T. The condition "much greater" is critical, as even for initial molar ratios $[HF] : B_T = 4 : 1$, nearly 4 moles of fluorine per mole of boron may be consumed, if a large fraction of BF_4^- is formed during the reaction (see discussion in Wamser, 1948, 1951). Hence without a substantial $[HF]$ excess over B_T, the rate may slow down significantly in the course of the reaction as $[HF]$ drops. Note that in such cases, the final equilibrium extent of hydrolysis and product/reactant ratio (Eq. (12)) is given by the final, not initial, $[HF]$ (cf. Table V, Wamser, 1948).

With the above assumptions, the characteristic (e-folding) time τ for the reaction may be calculated as (Appendix B):

$$\tau = (k_1[HF] + k_2)^{-1} \,. \tag{17}$$

Using k_1 and k_2 values derived from Wamser (1948, 1951) (Eqs. (15) and (16)), the calculated time for 99% equilibration ($t_{99\%} = -\ln(0.01) \times \tau$) is less than ~1 min for $[HF] > 0.01$ M

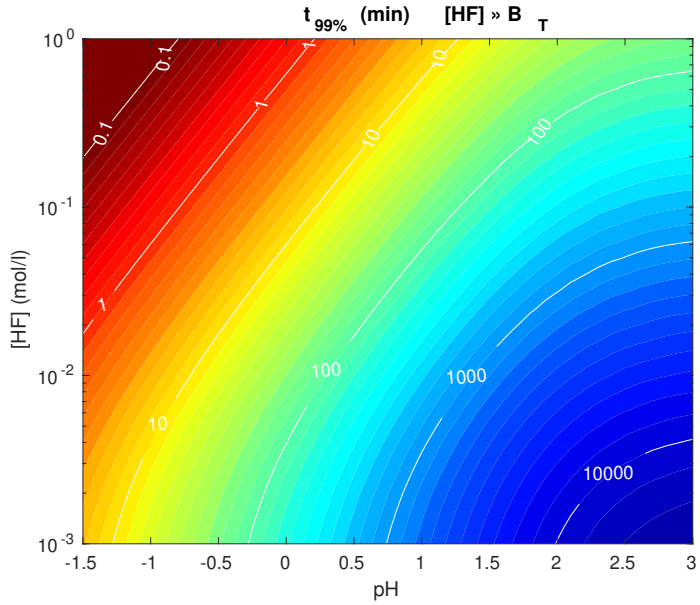

Figure 3. Calculated time for 99% equilibration of reaction (13) at 25°C, assuming [HF] to be much greater than the total boron concentration B_T (see text).

and $[H^+] > 1$ M due to acid catalysis (Fig. 3). However, $t_{99\%}$ increases dramatically to over 10,000 min (167 h) at low [HF] and pH > 2. Thus, the equilibration time is very sensitive to [HF] and pH. We note, however, that the specific numbers presented here should be taken with caution due to the limited available experimental studies on the subject and the disagreement between them (discussed above).

4 Isotopic Equilibrium: Theory

Isotopic fractionation factors in thermodynamic equilibrium are calculated from first principles based on differences in the vibrational energy of molecules. In this study, we determine fundamental frequencies and molecular forces using quantum-chemical (QC) computations (e.g. Jensen, 2004; Schauble, 2004; Zeebe, 2005; Guo et al., 2009; Rustad et al., 2010; Zeebe, 2014). Fractionation factors were calculated from reduced partition function

ratios (Urey, 1947):

$$\left(\frac{Q'}{Q}\right)_{\mathrm{r}} = \frac{s}{s'} \prod_i \frac{u'_i}{u_i} \frac{\exp(-u'_i/2)}{\exp(-u_i/2)} \frac{1-\exp(-u_i)}{1-\exp(-u'_i)}\,, \tag{18}$$

with s and s' being symmetry numbers, $u_i = hc\omega_i/kT$ and $u'_i = hc\omega'_i/kT$ where h is Planck's constant, c is the speed of light, k is Boltzmann's constant, T is temperature in Kelvin, and ω_i and ω'_i are the frequencies of the isotopic molecules or the solute-water clusters. Note that Eq. (18) is based on the harmonic approximation and hence requires harmonic ω's as input (see discussion in Zeebe (2005)), which we calculate here using QC calculations. In contrast, observed ω's include anharmonicity but will nevertheless be compared to harmonic ω's (see Section 5.1). In the present case, errors introduced by anharmonicity (e.g., Zeebe, 2005) are likely much smaller than those due to different QC methods (see below). The theoretical calculations yield β-factors, which, for a compound A is given by:

$$\beta_{\mathrm{A}} = \left(\frac{Q'_{\mathrm{A}}}{Q_{\mathrm{A}}}\right)_{\mathrm{r}}^{\frac{1}{k}}\,, \tag{19}$$

where k is the number of atoms being exchanged ($k = 1$ for boron in the compounds considered here). Finally, the fractionation factor α between two compounds A and B is given by:

$$\alpha_{(\mathrm{A-B})} = \frac{\beta_{\mathrm{A}}}{\beta_{\mathrm{B}}}\,.$$

4.1 Quantum-chemical computations

We used the quantum-chemical software package GAMESS, Sep-2018-R3 (Gordon and Schmidt, 2005) and different computational methods (differing in level of theory, LoT, and basis sets) to determine geometries and frequencies of key compounds in the boric acid – hydrofluoric acid system (Fig. 1). A very basic but fast method (HF/6-31G(d), HFb for

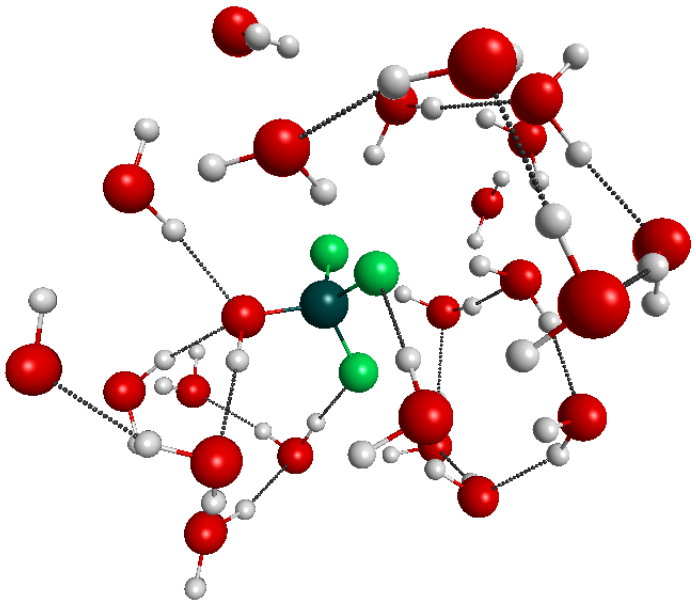

Figure 4. Solute-water cluster example. Optimized geometry of a hydrated $BF_3(OH)^-$ ion including 22 water molecules (C_1 symmetry) based on X3LYP/6-311+G(d,p) calculated with GAMESS (Gordon and Schmidt, 2005). Dark-green: boron, light-green: fluorine, red: oxygen, white: hydrogen. Dotted lines indicate hydrogen bonds.

short) was used for initial guesses and pre-optimization (for methods, see e.g., Jensen, 2004; Gordon and Schmidt, 2005). However, α's and β-factors obtained with HFb should be taken with caution because the method has limited accuracy. The density functional theory (DFT) method X3LYP/6-311+G(d,p) (X3LYP+) was employed for higher level optimizations and large solute-water clusters with up to $n = 22$ water molecules (Fig. 4). Computations with the most complete basis sets tested here were performed with MP2/aug-cc-pVDZ and MP2/aug-cc-pVTZ (MP2DZ, MP2TZ), which are however computationally expensive and mostly impractical for large solute-water clusters.

We selected the methods HFb, X3LYP+, and MP2TZ because they are frequently used in QC computations and similar LoT and basis sets have been applied to boron isotope calculations previously (e.g. Oi, 2000; Zeebe, 2005; Liu and Tossell, 2005; Rustad et al., 2010).

Also, X3LYP+ and MP2TZ yield values for $\alpha_{(B(OH)_3-B(OH)_4^-)}$ that cluster around the upper and lower end of the spectrum (Rustad et al., 2010). However, even for isolated ("gas-phase") molecules (see below), the higher-level DFT and MP2 methods differed by up to 5‰ in α's (Table 2). Given these differences, we refrain from testing further QC methods, which will unlikely narrow down the range of α values. The selected LoT and basis set therefore represents the largest uncertainty in our calculations, whereas the effect of hydration on the calculated boron isotope fractionation turned out to be less significant in most cases (see below).

For HFb and MP2DZ frequencies, scale factors of $s = 0.92$ and 1.03 were applied, whereas unscaled frequencies were used from X3LYP+ and MP2TZ computations. The scale factors applied here are close to those obtained from general low-frequency fits to >1,000 observed frequencies and are consistent with scale factors from our previous work on boron, carbon, and oxygen isotopes (Scott and Radom, 1996; Merrick et al., 2007; Zeebe, 2005, 2014). For all molecules and solute-water clusters studied here (see Figs. 1 and 4), geometry optimizations were followed by full Hessian (force-constant matrix) runs to determine frequencies and to ensure that none of the calculated frequencies was imaginary (geometrically unstable, e.g., HBF_4 at C_{2v} symmetry, see Fig. 1).

As mentioned above, the notations $BF_3(H_2O)$ and $HBF_3(OH)$ are used synonymously here (see Fig. 1). Note that initial geometries in which one hydrogen was positioned near any of the three F atoms quickly evolved into separate $BF_2(OH)^-$ and HF structures. This was the case for the isolated $HBF_3(OH)$ molecule, as well as for a hydrated unit including $n = 6$ water molecules. The B-O distance, which is large in $BF_3(H_2O)$ (∼1.84 Å, Fig. 1), is substantially smaller in the $BF_3(H_2O) \cdot (H_2O)_6$ cluster (∼1.54 Å) (both at X3LYP/6-311+G(d,p) level).

4.2 Uncertainties in computed α's

The range in the computed fractionation factors from the higher-level DFT and MP2 methods is reported here as an uncertainty estimate, as different QC methods yield significantly different values for α (see below). Other approaches have been used in the literature. For instance, propagated uncertainties in the computed frequencies derived for well-studied small molecules have been used as an error estimate for a single QC method (e.g., Kowalski et al., 2013). This approach is based on the well known tendency of certain methods to systematically under- or overestimate frequencies. However, this is a systematic, not random error (commonly corrected for by a scale factor, see Section 4.1), which says little about the QC method's accuracy when applied to a specific system for which experimental frequencies and α's are yet lacking. (Note that a QC method's precision for a fixed geometry is undefined as one method yields exactly one set of frequencies and one α value for that case.) Furthermore, it is not uncommon that certain QC methods give large errors in only a few (but critical) frequencies that deviate substantially from errors accounted for by an average frequency scaling. Also, the computed α value and its error for a given method is sensitive to the calculated frequency ***shift*** upon isotopic substitution, which is not necessarily related to the average error in absolute frequency for that method.

Alternatively, by averaging results from different QC methods, a "theoretical mean" α has been calculated to report its $\pm 1\sigma$ standard deviation as error (e.g., Li et al., 2020). However, it is important to realize that selected QC methods and their numerical results do not represent a set whose statistical sample mean approaches "a true mean value" for large N. Rather, the set of QC methods included in the analysis is an often arbitrary selection made by the

investigator, which inevitably leads to bias (some studies, for example, only include density functional theory methods). Furthermore, it is not clear whether results from methods with known limited accuracy such as HF/6-31G(d) should be included or not, which may be highly problematic in some cases, but inconsequential in others (HF/6-31G(d) fortuitously yields acceptable α values in several cases). For the various reasons outlined above, the uncertainty estimate reported here is given as the range in the computed α from different methods. We include results from the higher-level DFT and MP2 methods and exclude results from HF/6-31G(d).

5 Boron Isotope Partitioning

Given the dominant aqueous species discussed in Section 2, our calculations of boron isotope fractionation factors (α's) will mainly focus on $B(OH)_3$, $B(OH)_4^-$, BF_4^-, and $BF_3(OH)^-$. Of those compounds, the fractionation between $B(OH)_3$ and $B(OH)_4^-$ in aqueous solution has been established theoretically and experimentally and is described elsewhere (e.g. Zeebe, 2005; Liu and Tossell, 2005; Klochko et al., 2006; Rustad et al., 2010; Nir et al., 2015). To provide insight into the systematics of boron fractionation, we also include BF_3 for comparison between $\alpha_{(BF_3-BF_4^-)}$ and $\alpha_{(B(OH)_3-B(OH)_4^-)}$ (α_{BF34} and α_{34} for short), and HBF_4 and $HBF_3(OH)$ to assess the effect of protonation on α's.

5.1 Gas phase estimates

It is instructive to consider first quantum-chemical calculations for isolated ("gas-phase") molecules to gain an overview of α's in the boric–hydrofluoric acid system and to examine differences between levels of theory. It turned out that isolated HBF_4 was geometrically unstable at all LoT tested here, i.e., either one calculated frequency was imaginary (C_{2v}

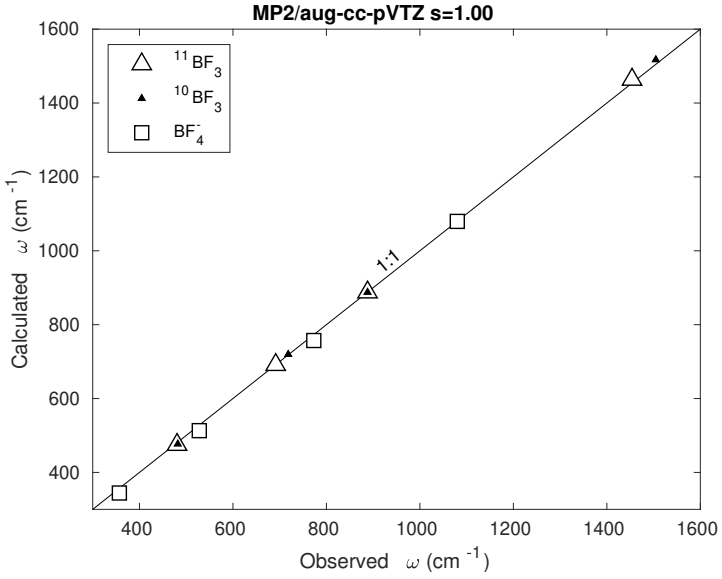

Figure 5. Calculated vs. observed fundamental frequencies of BF_3 and BF_4^- (Vanderryn, 1959; Nakane and Ōyama, 1966; Bates et al., 1971). Calculated ω's obtained at MP2/aug-cc-pVTZ level are unscaled ($s = 1.0$).

symmetry, Fig. 1), or the geometry optimization led to $BF_3 + HF$, suggesting that HBF_4 should not exist in the gas phase (Fărcasiu and Hâncu, 1997; Otto, 1999). Starting with HBF_4 in C_{2v} symmetry, adding two H_2O molecules ($HBF_4 \cdot (H_2O)_2$), and then removing all symmetry restrictions in the calculation (C_1), led to disintegration into a $BF_3 - FH - (H_2O)_2$ configuration, in which BF_3 was slightly non-planar (tested with HF/6-31G(d)). An alternative configuration (C_1) that resembled $BF_4^- - H_3O^+ - H_2O$ was geometrically stable at all LoT tested here.

The calculated fundamental molecular frequencies (ω's) and their shift upon isotopic substitution are key to evaluate Eq. (18). Measured ω's are available, e.g., for BF_3 (Vanderryn, 1959; Nakane and Ōyama, 1966) and BF_4^- from $NaBF_4$ in aqueous solution (Bates et al., 1971) and can be compared to calculated frequencies from our quantum-chemical computations (Fig. 5). The match is quite good at the highest LoT tested here (MP2/aug-cc-pVTZ) — the

calculated ω's line up close to the 1:1 line without scaling (scale factor $s = 1$). At a basic LoT (HF/6-31G(d)) the asymmetric stretch in BF_3 at ~1450 cm^{-1} falls slightly below the 1:1 line, while the asymmetric stretch in BF_4^- at ~1100 cm^{-1} falls above the 1:1 line ($s = 0.92$, not shown). As a result, the β-factors of BF_3 and BF_4^- are probably too small and too large, respectively, and hence α_{BF34} at HF/6-31G(d) is likely underestimated (Fig. 6, Table 2, see Electronic Annex).

Despite differences between LoT and basis sets, a few patterns emerge from our calculations that appear robust. First, all B-F compounds considered are enriched in ^{11}B relative to $B(OH)_4^-$ (Fig. 6). Second, BF_3 and BF_4^- are isotopically heavier than $B(OH)_3$ and $B(OH)_4^-$, respectively, indicating that boron is more strongly bound in the B-F than the B-OH compounds, given the pairwise similar molecular geometries (D_{3h} vs. C_{3h} and T_d vs. S_4 symmetry). The order of ^{11}B enrichment may have been expected from bond strength and bond length (d) of B-F vs. B-O in these compounds (e.g., $d_{B-F} \simeq 1.31$ Å in BF_3, $d_{B-O} \simeq 1.37$ Å in $B(OH)_3$). Furthermore, the β-factor of $BF_3(OH)^-$ falls below or close to that of BF_4^- and the effect of protonation is small (compare, e.g., fractionation between $BF_3(OH)^-$ and $HBF_3(OH)$, see Fig. 6).

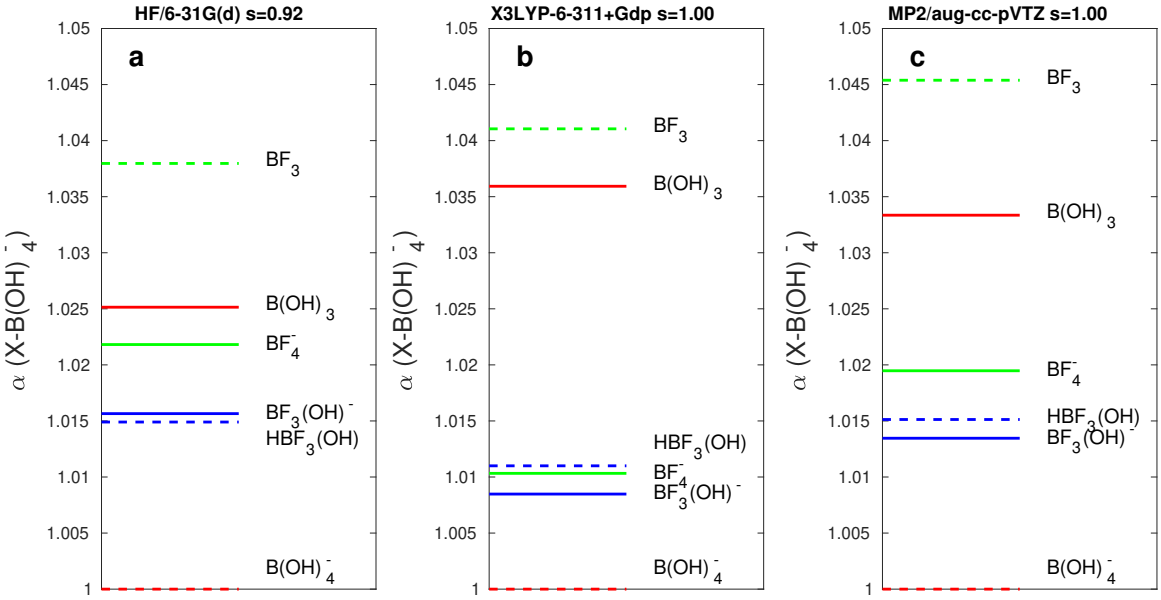

Figure 6. Calculated stable boron isotope fractionation of selected compounds in the boric acid – hydrofluoric acid system at 25°C relative to $B(OH)_4^-$. The level of theory and size of the basis set increase from a to c.

Table 2. Calculated gas phase β-factors and α's at 25°C (see Electronic Annex). [a]

	HFb	X3LYP+	MP2TZ
		β	
$B(OH)_3$	1.2313	1.2340	1.2363
$B(OH)_4^-$	1.2011	1.1913	1.1964
BF_3	1.2467	1.2401	1.2507
BF_4^-	1.2273	1.2035	1.2197
$BF_3(OH)^-$	1.2199	1.2013	1.2125
$HBF_3(OH)$[b]	1.2190	1.2043	1.2145
HBF_4	**I**[c]	**I**	**I**
$BF(OH)_3^-$			1.2002
$BF_2(OH)_2^-$			1.2057
		α	
α_{34}	1.0252	1.0358	1.0333
α_{BF34}	1.0158	1.0304	1.0254

[a]HFb = HF/6-31G(d), X3LYP+ = X3LYP/6-311+G(d,p), MP2TZ = MP2/aug-cc-pVTZ with scale factors $s = [0.92\ 1.00\ 1.00]$.

[b]$HBF_3(OH) = BF_3(H_2O)$.

[c]**I** = one ω imaginary (geometrically unstable, see text).

The details of the calculated β-factors and α's depend, however, on the LoT and basis sets used (see Fig. 6 and Table 2). For instance, the order of boron isotope enrichment in $HBF_3(OH)$ vs. $BF_3(OH)^-$ is reversed for HFb, compared to X3LYP+ and MP2TZ (Fig. 6). Considering only the higher-level DFT and MP2 methods, BF_4^- is enriched in ^{11}B relative to $B(OH)_4^-$ by ~10‰ for X3LYP+ but by ~20‰ for MP2TZ, respectively. The two methods differ by 5‰ in $\alpha_{(BF_3-BF_4^-)}$ (see Table 2). Selection of the QC method (level of theory and basis set) thus represents the largest uncertainty in our isotope calculations for most compounds (cf. Section 5.2).

5.2 Solute-water clusters

We also performed geometry optimizations and Hessian (force-constant matrix) runs for large solute-water clusters with up to $n = 22$ water molecules using the density functional theory (DFT) method X3LYP/6-311+G(d,p) (X3LYP+) (cf. Fig. 4). MP2/aug-cc-pVDZ and MP2/aug-cc-pVTZ (MP2DZ and MP2TZ) are computationally too expensive and mostly impractical for large solute-water clusters (we tested MP2DZ for $n \leq 6$). It turned out that the effect of hydration on the calculated β-factors for boron isotope exchange is minor in most cases, except for BF_4^- and $B(OH)_3$ (Fig. 7). For instance, the hydration effect reduces $\alpha_{(B(OH)_3-B(OH)_4^-)}$ by ~6‰ at 25°C as n increases from 0 to 20 for X3LYP+ (included in our calculations on temperature dependence, see Section 5.4). However, the effect of hydration is much smaller in most other cases and, importantly, less significant for MP2DZ than for X3LYP+ (Fig. 7), suggesting that our "gas-phase" estimates from MP2TZ are reasonable approximations to boron isotope fractionation in aqueous solution in most cases (Table 2). Clearly, the overall uncertainties introduced by different QC methods (Fig. 6) are substantially larger than those resulting from hydration, except for BF_4^- and $B(OH)_3$ at X3LYP+ (Fig. 7).

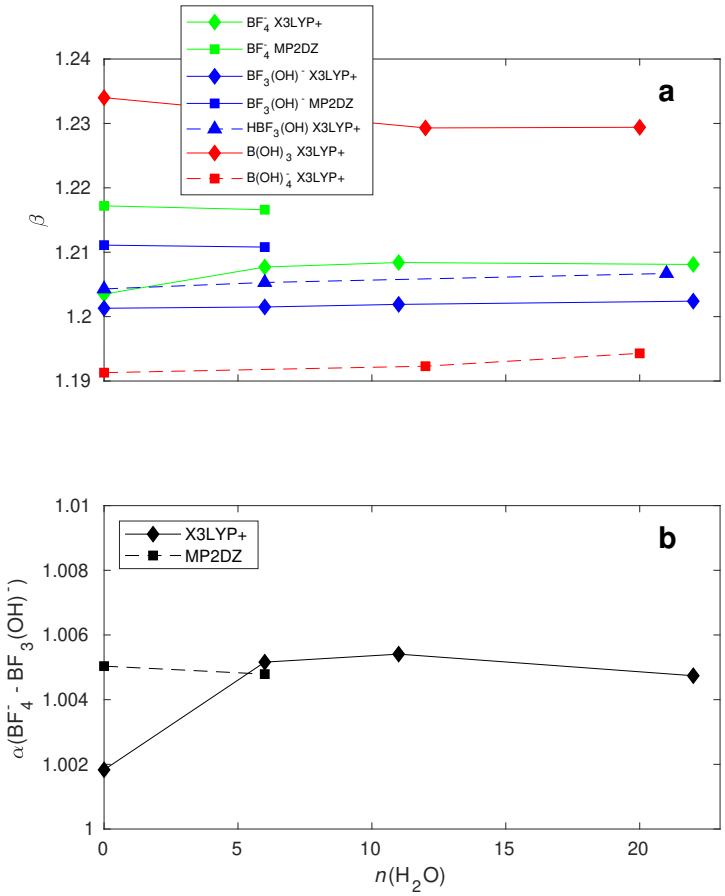

Figure 7. Selected β-factors and $\alpha_{(BF_4^- - BF_3(OH)^-)}$ from computations including solute-water clusters with up to $n = 22$ water molecules.

5.3 Boron isotope partitioning vs. pH

Given the calculated fractionation factors (α's) between the various compounds (e.g., Table 2) and the speciation vs. pH (Fig. 2), the boron isotope partitioning in the boric acid – hydrofluoric acid system as a function of pH can be calculated. The correct mass balance calculation uses fractional abundances rather than isotope ratios, R's (e.g., Hayes, 1982). However, the difference is at most 0.15‰ in the present case (see Appendix C). Using R's, a

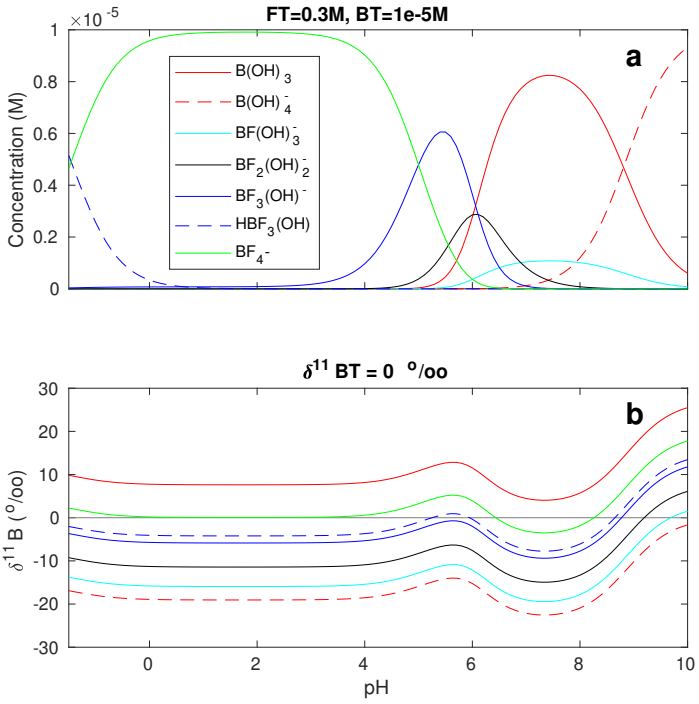

Figure 8. Speciation and boron isotope partitioning in the boric acid – hydrofluoric acid system at 25°C. (a) Note that $[HBF_3(OH)]$ is uncertain as only estimated values for pK'_3 are available. (b) The boron isotope composition of total boron (B_T) in the systen was set to $\delta^{11}B_T = 0‰$.

general isotope mass balance at any given pH may be written as:

$$R_T X_T = \sum R_i c_i \,, \tag{20}$$

where index T refers to 'Total', and X_T and c_i are the total inventory and individual concentrations of compounds containing element X, respectively. If we express all α's relative to a single compound A, we can write $R_i = \alpha_i R_A$. Then,

$$R_T X_T = R_A \sum \alpha_i c_i \,, \tag{21}$$

which can be solved for R_A:

$$R_A = R_T X_T / \sum \alpha_i c_i \,. \tag{22}$$

All remaining R's are calculated from $R_i = \alpha_i R_A$. These expressions were evaluated at 25°C using MP2TZ-calculated values for most α's (Table 2), the experimental α_{34} (Klochko et al., 2006), and $\delta^{11}B_T = 0‰$ (Fig. 8). The β-factors of $BF(OH)_3^-$ and $BF_2(OH)_2^-$ at MP2TZ level were calculated as 1.2002 and 1.2057 (Table 2). The concentrations of the protonated forms $HBF(OH)_3$, etc., are very small and make virtually no difference, except for $HBF_3(OH)$ at very low pH. The β-factors of the protonated forms were taken equal to the corresponding non-protonated forms. As expected, over the pH range where BF_4^- dominates, the $\delta^{11}B$ of BF_4^- is close to $\delta^{11}B_T = 0‰$. The boron isotope partitioning only shifts above $p\mathrm{H} \simeq 4$, first towards $BF_3(OH)^-$, then $B(OH)_3$, and finally $B(OH)_4^-$, having respective $\delta^{11}B$ values close to $\delta^{11}B_T$ (Fig. 8).

5.4 Effect of temperature

Given that the effect of hydration on boron fractionation for most B-F compounds is small relative to the effect of different LoT (Fig. 7), we calculated the temperature dependence of $\alpha_{(BF_3-BF_4^-)}$ based on isolated molecules at the highest LoT tested here (MP2/aug-cc-pVTZ, Fig. 9). For $\alpha_{(B(OH)_3-B(OH)_4^-)} = \alpha_{34}$ we use results from our X3LYP/6-311+G(d,p) calculations of solute-water clusters with $n = 20$. We also include an α_{34}^*, which uses the measured α_{34} seawater value at 25°C (Klochko et al., 2006) and an estimated temperature dependence based on the slope of our calculated α_{34} scaled by the ratio $\alpha_{34}^*/\alpha_{34}$ at 25°C (Fig. 7). From 0 to 40°C, the calculated α's are very nearly linear vs. temperature for which we provide a fit of the form:

$$\varepsilon = (\alpha - 1)10^3 = \varepsilon_{25} + \lambda \cdot (T_C - 25)\,, \tag{23}$$

where T_C is temperature in °C. From 0 to 300°C, we use a fit of the form:

$$\varepsilon = a + b/T + c/T^2, \tag{24}$$

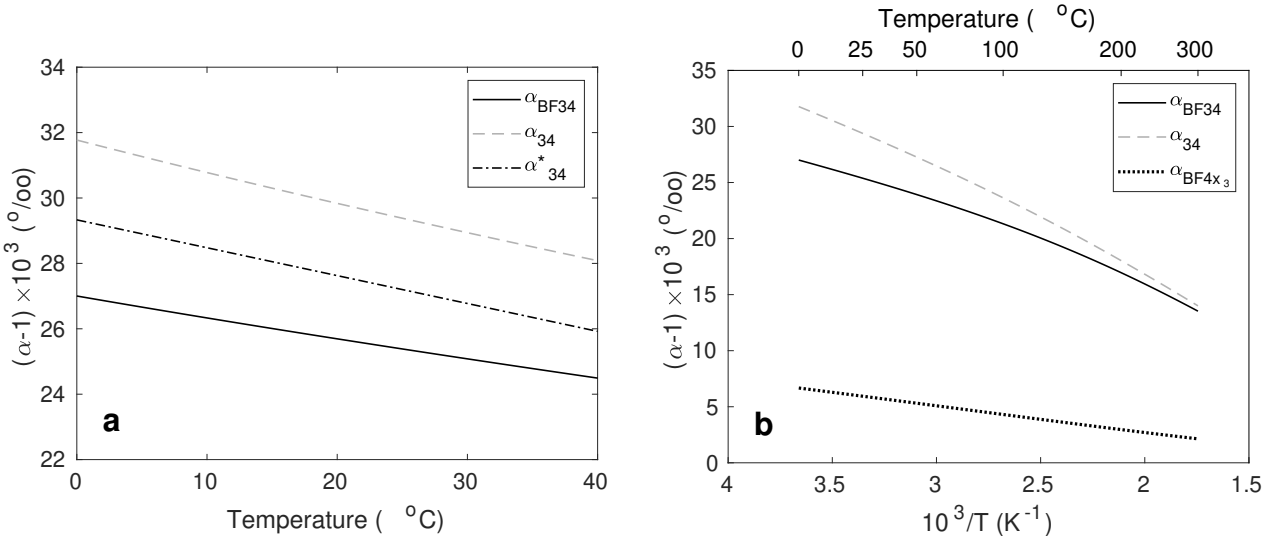

Figure 9. Temperature dependence of α's. $\alpha_{BF34} = \alpha_{(BF_3-BF_4^-)}$ at MP2/aug-cc-pVTZ level; $\alpha_{34} = \alpha_{(B(OH)_3-B(OH)_4^-)}$ from X3LYP/6-311+G(d,p) calculations of solute-water clusters with $n = 20$. (a) α^*_{34} uses the measured α_{34} seawater value at 25°C (Klochko et al., 2006) and the slope of the calculated α_{34} (dashed line) scaled by the ratio $\alpha^*_{34}/\alpha_{34}$ at 25°C. (b) $\alpha_{BF_4x_3} = \alpha_{(BF_4^- - BF_3(OH)^-)}$.

where T is temperature in Kelvin (for fit coefficients, see Table 3). The maximum errors of our fits are less than ∼0.15‰.

Table 3. Coefficients for temperature fits Eqs. (23) and (24).

	ε_{25}	λ	a	$b\times10^{-3}$	$c\times10^{-6}$	Notes
$\alpha_{(BF_3-BF_4^-)}$	25.4	−0.0627	−7.3143	14.3867	−1.3806	‡
$\alpha_{(B(OH)_3-B(OH)_4^-)}$	29.4	−0.0921	−8.9720	15.0475	−1.0757	#
$\alpha^*_{(B(OH)_3-B(OH)_4^-)}$	27.2	−0.0852				&

‡MP2/aug-cc-pVTZ.
#X3LYP/6-311+G(d,p), $n = 20$.
&See text.

6 Best Practice in Boron Analyses with HF Addition

Recently, it has been shown that addition of hydrofluoric acid can improve washout times of boron in the introduction systems of (MC-)ICPMS instruments (Misra et al., 2014b; Rae et al., 2018; He et al., 2019). Slow washout of boron results from the volatility of $B(OH)_3$ (Brenner and Cheatham, 1998), which can be entrained from droplets coating the walls of ICPMS spray chambers (Al-Ammar et al., 1999), leading to persistence of up to 50% of the initial signal after ∼5 min of wash, and associated memory effects between samples and standards.

Previously, addition of ammonia gas to the spray chamber has been used to help combat this issue, leading to improved signal memory of 2% after ∼3 min wash (Al-Ammar et al., 2000; Foster, 2008). This result can be explained by conversion of volatile boric acid to non-volatile borate ion at elevated pH. Notably, as samples, standards, and blanks are introduced in 0.5 M HNO_3, and as the ∼3 ml min^{-1} NH_3 gas flux is diluted in the spray chamber by ∼1 l min^{-1} Ar, the bulk solution in the spray chamber remains acidic ($pH < 1$ when tested). We therefore suggest that the suppression of boron volatility caused by NH_3 addition results from pronounced elevation of pH (to greater than the boric acid $pK \simeq 9$) on the surface layer (and perhaps in the aqueous diffusion boundary layer) of otherwise acidic droplets.

Addition of HF offers an alternative method of improving boron washout. This was first noted by Makishima et al. (1997) and studied in more detail by Misra et al. (2014b,a); Rae et al. (2018); He et al. (2019). The examination of boron partitioning here allows us to provide further insights into best practice in boron analysis in an HF matrix. Avoiding the presence of volatile $B(OH)_3$ requires that all boric acid is converted to fluoroboric species.

This requires an excess of F^- ions over total boron, which is found with a combination of low pH, high total fluorine, and low total boron (Fig. 2). Boron is typically analyzed at sub-ppm concentrations in geochemistry, so overly high boron concentrations are unlikely to present an issue (cf. Fig. 2c). However, relatively high total concentrations of HF are needed to ensure complete consumption of $B(OH)_3$ (Fig. 2b). This is a function of HF's pK ($\sim$3), which means that at $p\mathrm{H} = 1$, only $\sim$1% of total fluorine is present as free F^- (Eq. (10)). Low pH (< 5) is also required (Fig. 2a), which is typical in geochemical analyses, and cautions against attempting to use HF and NH_3 in combination to reduce boron washout.

The kinetics of $B(OH)_3$ reaction with HF are generally fast, except for the formation of the final product, BF_4^- (reaction (13)). As a result, volatile $B(OH)_3$ may still be present in solutions to which HF has recently been added. As well as reducing the efficiency of the washout, this has the potential to impart isotopic fractionation, via preferential loss of the isotopically heavy trigonal $B(OH)_3$. To avoid this, solutions should have HF added in advance of analysis depending on pH and [HF] (see Fig. 3). Slow conversion to BF_4^- may also limit the efficiency of washout if HF is used only as a rinse solution rather than being added to the analytes.

The current procedure in the STAiG laboratory at the University of St Andrews is to run MC-ICPMS boron isotope analyses in 0.5 M HNO_3 + 0.3 M HF (see Rae et al., 2018). This matrix is used for all solutions — standards, samples, and blanks — and results in washout to $\sim$0.5% in 3 minutes (cf. $\sim$3% when using NH_3 gas). Samples, initially in 0.5 M HNO_3 following chemical purification, are "spiked" with a small volume of concentrated HF (to avoid dilution) about 1/2 hour prior to analysis (the estimated 99% equilibration time at this pH and HF content is $\sim$10 minutes, see Fig. 3). Maintaining a constant matrix for all solutions in the run is generally desirable to avoid differences in mass bias or background

contamination, though we note that solutions of the standard NIST 951 run as test samples with HF concentrations ranging from 0 to 0.5 M show no systematic differences. For analysis of trace boron concentrations, however, we use HF only in the wash solution. We do not add HF to our trace element samples, despite the potential further improvement in washout, due to the lower overall boron concentrations, higher throughput of samples, risk of contamination of other elements, and reduced contribution of boron washout to precision. Also note that HF should not be added to samples that are to be separated by ion exchange chromatography with Amberlite 743, as BF_4^- does not interact well with this resin.

Alongside the improved washout, use of HF also has advantages over NH_3 in terms of machine sensitivity, avoiding a signal decrease of $\sim$10-20% with NH_3, and stability and run times, avoiding build-up of ammonium nitrate salts in the injector. The main drawback of HF use is the safety hazard, requiring careful operating procedures (for instance use of neoprene rather than nitrile gloves), though note that a 0.3 M solution is equivalent to a $\sim$1% dilution, considerably less hazardous than fully concentrated HF (29 M). Hydrofluoric acid use also requires an "inert" sample introduction kit, including self-aspirating Teflon nebulizers, Teflon spray chambers, and sapphire injectors.

7 Summary and Conclusions

In the present study, we have examined the equilibria and kinetics in the aqueous boric acid – hydrofluoric acid system using available experimental data. We have presented the first quantum-chemical computations to determine boron isotope fractionation in the fluoroboric acid system and have provided suggestions on best practice in the application of HF in experimental boron analyses. Our results show that at low pH ($0 \leq p\text{H} \leq 4$) and for total fluorine (F_T) much greater than total boron (B_T), the dominant aqueous species is BF_4^-.

Our estimated time for 99% equilibration ($t_{99\%}$) of the slowest reaction in the system (forming BF_4^-) is less than ~1 min at constant [HF] > 0.01 M and [H^+] > 1 M, assuming $F_T \gg B_T$. However, $t_{99\%}$ increases dramatically to over 167 h at low [HF] and pH > 2, suggesting that the equilibration time is very sensitive to [HF] and pH. Our quantum-chemical (QC) computations suggest that the equilibrium boron isotope fractionation between BF_3 and BF_4^- is slightly smaller than that calculated between $B(OH)_3$ and $B(OH)_4^-$. Yet, BF_4^- is enriched in ^{11}B relative to $B(OH)_4^-$ in all our calculations ($\alpha_{(BF_4^- - B(OH)_4^-)} > 1.0$), regardless of the QC method tested. Unfortunately, even considering only the higher-level QC methods tested, the calculated α values differ by ~10‰ in $\alpha_{(BF_4^- - B(OH)_4^-)}$ and by ~5‰ in $\alpha_{(BF_3 - BF_4^-)}$. Selection of the QC method (level of theory and basis set) thus represents the largest uncertainty in our isotope calculations for most compounds. The effect of hydration on the calculated boron isotope fractionation is much smaller in most cases, except for BF_4^- and $B(OH)_3$ computed with the density functional theory method X3LYP/6-311+G(d,p).

The results of our study should be helpful for implementing and advancing geochemical applications in high precision analyses of boron concentration and isotopic composition. One specific application is the addition of hydrofluoric acid to boron samples, which has recently been shown to improve washout times of boron in the introduction systems of (MC-)ICPMS instruments. However, beyond geochemical applications, our study should serve as a general resource for a variety of studies dealing with equilibria, kinetics, and boron isotope fractionation in the aqueous boric acid – hydrofluoric acid system, including applications in physical chemistry, polymer science, sandstone acidizing, and more.

Acknowledgments. To be added.

Appendix A: Equilibrium speciation

To simplify the calculations, we use in the following $x_i = [\mathrm{BF_i(OH)_{4-i}^-}]$, $y_i = [\mathrm{HBF_i(OH)_{4-i}}]$ $(i = 1, \ldots, 4)$, $b_3 = [\mathrm{B(OH)_3}]$, $b_4 = [\mathrm{B(OH)_4^-}]$, $f = [\mathrm{F^-}]$, $g = [\mathrm{HF}]$, $h = [\mathrm{H^+}]$, and $L_i = 1/K_i'$. Using equilibrium relationships (see Section 2), we can thus write: $y_i = x_i h L_i$, $g = f h L_F$, and $b_4 = b_3\, K_B/h$. Given pH, total boron (B_T) and total fluorine (F_T), the mass balance equations read:

$$\mathrm{B}_T = b_3(1 + K_B/h) + \sum x_i(1 + hL_i) \tag{A1}$$

$$\mathrm{F}_T = f(1 + hL_F) + \sum i\, x_i(1 + hL_i)\,, \tag{A2}$$

in which we substitute x_i's using K_i's (Eqs. (5) and (6)):

$$\mathrm{B}_T = b_3\,[1 + K_B/h + \sum a_i(1 + hL_i)f^i] \tag{A3}$$

$$\mathrm{F}_T = f(1 + hL_F) + b_3 \sum i a_i(1 + hL_i)f^i\,, \tag{A4}$$

with $a_1 = K_1$, $a_2 = K_2 h$, $a_3 = K_3 h^2$, $a_4 = K_4 h^3$, and eliminate b_3:

$$\mathrm{B}_T \sum i a_i(1 + hL_i)f^i = [\mathrm{F}_T - f(1 + hL_F)][1 + K_B/h + \sum a_i(1 + hL_i)f^i]\,. \tag{A5}$$

This expression can be solved numerically for f at given pH. b_3 can now be obtained from Eq. (A3), all x_i determined from Eqs. (5) and (6), and all y_i from $y_i = x_i h L_i$.

Appendix B: Analytical solution of kinetic rate equation

The kinetic rate equation (14):

$$\frac{\mathrm{d}[\mathrm{BF}_4^-]}{\mathrm{d}t} = k_1[\mathrm{BF}_3(\mathrm{OH})^-][\mathrm{HF}] - k_2[\mathrm{BF}_4^-] \tag{B6}$$

can be solved analytically with some critical assumptions. We assume low pH where $[\mathrm{BF}_3(\mathrm{OH})^-]$ and $[\mathrm{BF}_4^-]$ are the dominant B-F species, hence we set $\mathrm{B}_T = [\mathrm{BF}_3(\mathrm{OH})^-] + [\mathrm{BF}_4^-]$. Furthermore, we assume constant $[\mathrm{H}^+]$ and $[\mathrm{HF}]$ during the reaction, which should hold approximately for $\mathrm{F}_T \gg \mathrm{B}_T$. Then:

$$\frac{\mathrm{d}[\mathrm{BF}_4^-]}{\mathrm{d}t} = k_1(\mathrm{B}_T - [\mathrm{BF}_4^-])[\mathrm{HF}] - k_2[\mathrm{BF}_4^-] \tag{B7}$$

$$= -(k_1[\mathrm{HF}] + k_2)[\mathrm{BF}_4^-] + k_1\mathrm{B}_T[\mathrm{HF}] = -k[\mathrm{BF}_4^-] + \gamma\,, \tag{B8}$$

where $k = (k_1[\mathrm{HF}] + k_2) = \tau^{-1}$ is the overall rate constant (inverse characteristic time scale) and $\gamma = k_1\mathrm{B}_T[\mathrm{HF}]$ is a constant. The solution is:

$$[\mathrm{BF}_4^-](t) = ([\mathrm{BF}_4^-]_0 - \gamma/k)\ \exp(-kt) + \gamma/k\,, \tag{B9}$$

where index '0' indicates initial $[\mathrm{BF}_4^-]$ at $t = 0$ and $\gamma/k = (k_1\mathrm{B}_T[\mathrm{HF}])/(k_1[\mathrm{HF}] + k_2)$ equals $[\mathrm{BF}_4^-]$ in equilibrium, which can be shown using $k_2/k_1 = K_h = [\mathrm{BF}_3(\mathrm{OH})^-]_{eq}[\mathrm{HF}]/[\mathrm{BF}_4^-]_{eq}$, as it should be. Our solution (Eq. (B9)) is similar to Eq. (4) of Fucskó et al. (1993), except that our solution allows for explicitly specifying $[\mathrm{BF}_4^-]_0$. The time evolution is given by the exponential term and hence the characteristic (e-folding) time $\tau = (k_1[\mathrm{HF}] + k_2)^{-1}$.

Appendix C: Isotope mass balance using fractional abundance

The correct isotope mass balance using fractional abundances (r's) reads (e.g., Hayes, 1982):

$$r_T X_T = \sum r_i c_i \,, \tag{C10}$$

where index T refers to 'Total', and X_T and c_i are the total inventory and individual concentrations of compounds containing element X, respectively. Using $r_i = R_i/(1+R_i)$ and expressing all α's relative to a single compound A, we can write $R_i = \alpha_i R_A$ and thus:

$$r_T X_T = \sum c_i R_i/(1+R_i) = \sum c_i \alpha_i R_A/(1+\alpha_i R_A) \,, \tag{C11}$$

which can be solved numerically for R_A. All remaining R's are calculated from $R_i = \alpha_i R_A$. In the present case, the result only differs from a mass balance using R's (Eq. 22) by at most 0.15‰.

References

Al-Ammar, A., Gupta, R. K., and Barnes, R. M. Elimination of boron memory effect in inductively coupled plasma-mass spectrometry by addition of ammonia. *Spectrochim. Acta B: Atomic. Spectr.*, 54 (7):1077–1084, 1999. doi: 10.1016/S0584-8547(99)00045-2.

Al-Ammar, A. S., Gupta, R. K., and Barnes, R. M. Elimination of boron memory effect in inductively coupled plasma-mass spectrometry by ammonia gas injection into the spray chamber during analysis. *Spectrochim. Acta B: Atomic. Spectr.*, 55(6):629–635, 2000.

Anbar, M. and Guttmann, S. The isotopic exchange of fluoroboric acid with hydrofluoric acid. *J. Phys. Chem.*, 64(12):1896–1899, 1960.

Bates, J. B., Quist, A. S., and Boyd, G. E. Infrared and Raman Spectra of Polycrystalline $NaBF_4$. *J. Chem. Phys.*, 54(1):124–126, 1971. doi: 10.1063/1.1674581.

Branson, O. Boron incorporation into marine $CaCO_3$. In Marschall, H. R. and Foster, G., editors, *Boron Isotopes, The Fifth Element*, pages 71–105. Springer, 2018.

Brenner, I. B. and Cheatham, M. M. Determination of boron: Aspects of contamination and vaporization. *ICP Inf. Newslett.*, 24:320, 1998. URL http://icpinformation.org.

De Hoog, J. C. M. and Savov, I. P. Boron isotopes as a tracer of subduction zone processes. In Marschall, H. R. and Foster, G., editors, *Boron Isotopes, The Fifth Element*, pages 189–215. Springer, 2018.

Fărcasiu, D. and Hâncu, D. Acid strength of tetrafluoroboric acid The hydronium ion as a superacid and the inapplicability of water as an indicator of acid strength. *J. Chem. Soc., Faraday Trans.*, 93(12): 2161–2165, 1997.

Foster, G. L. Seawater pH, pCO_2 and $[CO_3^{2-}]$ variations in the Caribbean Sea over the last 130 kyr: A boron isotope and B/Ca study of planktic foraminifera. *Earth Planet. Sci. Lett.*, 271:254–266, doi:10.1016/j.epsl.2008.04.015, 2008.

Fry, J. L., Orfanopoulos, M., Adlington, M. G., P, D. J. W., and Silverman, S. B. Reduction of aldehydes and ketones to alcohols and hydrocarbons through use of the organosilane-boron trifluoride system. *J. Org. Chem.*, 43(2):374–375, 1978.

Fucskó, J., Tan, S. H., La, H., and Balazs, M. K. Fluoride interference in the determination of boron by inductively coupled plasma emission spectroscopy. *Appl. Spectrosc.*, 47(2):150–155, 1993. doi: 10.1366/0003702934048181.

Gordon, M. S. and Schmidt, M. W. Advances in electronic structure theory: GAMESS a decade later. In G. Frenking, K. S. Kim, G. E. Scuseria, editor, *Theory and Applications of Computational Chemistry: the first forty years*, pages 1167–1189. Elsevier, Amsterdam, 2005.

Grassino, S. L. and Hume, D. N. Stability constants of mononuclear fluoborate complexes in aqueous solution. *J. Inorg. Nucl. Chem.*, 33(2):421–428, 1971.

Guinoiseau, D., Louvat, P., Paris, G., Chen, J.-B., Chetelat, B., Rocher, V., Guérin, S., and Gaillardet, J. Are boron isotopes a reliable tracer of anthropogenic inputs to rivers over time? *Sci. Tot. Env.*, 626: 1057–1068, 2018. doi: 10.1016/j.scitotenv.2018.01.159.

Guo, W., Mosenfelder, J. L., Goddard, I., William A., and Eiler, J. M. Isotopic fractionations associated with phosphoric acid digestion of carbonate minerals: Insights from first-principles theoretical modeling and clumped isotope measurements. *Geochim. Cosmochim. Acta*, 73(24):7203–7225, 2009. doi: 10.1016/j.gca.2009.05.071.

Hayes, J. M. Fractionation et al.: An introduction to isotopic measurements and terminology. *Spectra*, 8:3–8, 1982.

He, M.-Y., Deng, L., Lu, H., and Jin, Z.-D. Elimination of the boron memory effect for rapid and accurate boron isotope analysis by MC-ICP-MS using NaF. *J. Anal. Atom. Spectrom.*, 34(5):1026–1032, 2019.

Hönisch, B., Eggins, S. M., Haynes, L. L., Allen, K. A., Holland, K. D., and Lorbacher, K. *Boron Proxies in Paleoceanography and Paleoclimatology*. pp. 248, Wiley-Blackwell, 2019.

Jensen, F. *Introduction to computational chemistry*. Wiley, Chichester, UK, pp. 429, 2004.

Katagiri, J., Yoshioka, T., and Mizoguchi, T. Basic study on the determination of total boron by conversion to tetrafluoroborate ion (BF_4^-) followed by ion chromatography. *Analyt. Chim. Acta*, 570 (1):65–72, 2006.

Klochko, K., Kaufman, A. J., Yao, W., Byrne, R. H., and Tossell, J. A. Experimental measurement of boron isotope fractionation in seawater. *Earth Planet. Sci. Lett.*, 248(1-2):276–285, 2006. doi: 10.1016/j.epsl.2006.05.034.

Kowalski, P. M., Wunder, B., and Jahn, S. Ab initio prediction of equilibrium boron isotope fractionation between minerals and aqueous fluids at high P and T. *Geochim. Cosmochim. Acta*, 101: 285–301, 2013. doi: 10.1016/j.gca.2012.10.007.

Leong, V. H. and Ben Mahmud, H. A preliminary screening and characterization of suitable acids for sandstone matrix acidizing technique: a comprehensive review. *J. Petrol. Explor. Prod. Technol.*, 9(1): 753–778, 2019.

Li, X., Li, H.-Y., Ryan, J. G., Wei, G.-J., Zhang, L., Li, N.-B., Huang, X.-L., and Xu, Y.-G. High-precision measurement of B isotopes on low-boron oceanic volcanic rock samples via MC-ICPMS: Evaluating acid leaching effects on boron isotope compositions, and B isotopic variability in depleted oceanic basalts. *Chem. Geol.*, 505:76–85, 2019. doi: 10.1016/j.chemgeo.2018.12.011.

Li, Y.-C., Chen, H.-W., Wei, H.-Z., Jiang, S.-Y., Palmer, M. R., van de Ven, T. G. M., Hohl, S., Lu, J.-J., and Ma, J. Exploration of driving mechanisms of equilibrium boron isotope fractionation in tourmaline group minerals and fluid: A density functional theory study. *Chem. Geol.*, 536:119466, 2020. doi: 10.1016/j.chemgeo.2020.119466.

Lide, D. R. *CRC handbook of chemistry and physics*, volume 85. CRC press, 2004.

Liu, Y. and Tossell, J. A. Ab initio molecular orbital calculations for boron isotope fractionations on boric acids and borates. *Geochim. Cosmochim. Acta*, 69(16):3995–4006, 2005.

Makishima, A., Nakamura, E., and Nakano, T. Determination of boron in silicate samples by direct aspiration of sample hf solutions into icpms. *Anal. Chem.*, 69(18):3754–3759, 1997. doi: 10.1021/ac970383s.

Marschall, H. R. Boron isotopes in the ocean floor realm and the mantle. In Marschall, H. R. and Foster, G., editors, *Boron Isotopes, The Fifth Element*, pages 189–215. Springer, 2018.

Maya, L. Fluoroboric acid and its hydroxy derivatives–solubility and spectroscopy. *J. Inorg. Nucl. Chem.*, 39(2):225–231, 1977.

Merrick, J. P., Moran, D., and Radom, L. An Evaluation of Harmonic Vibrational Frequency Scale Factors. *J. Phys. Chem. A*, 111(45):11683–11700, 2007. doi: 10.1021/jp073974n.

Mesmer, R. E., Palen, K. M., and Baes Jr, C. F. Fluoroborate equilibria in aqueous solutions. *Inorg. Chem.*, 12(1):89–95, 1973.

Misra, S., Greaves, M., Owen, R., Kerr, J., Elmore, A. C., and Elderfield, H. Determination of B/Ca of natural carbonates by HR-ICP-MS. *Geochem., Geophys., Geosys.*, 15(4):1617–1628, 2014a.

Misra, S., Owen, R., Kerr, J., Greaves, M., and Elderfield, H. Determination of δ^{11}B by HR-ICP-MS from mass limited samples: Application to natural carbonates and water samples. *Geochim. Cosmochim. Acta*, 140:531–552, 2014b.

Nakane, R. and Ōyama, T. Boron Isotope Exchange between Boron Fluoride and Its Alkyl Halide Complexes. II. 1 Infrared Spectrum of Boron Fluoride-Methyl Fluoride Complex. *J. Phys. Chem.*, 70 (4):1146–1150, 1966.

Nir, O., Vengosh, A., Harkness, J. S., Dwyer, G. S., and Lahav, O. Direct measurement of the boron isotope fractionation factor: Reducing the uncertainty in reconstructing ocean paleo-pH. *Earth and Planetary Science Letters*, 414:1–5, 2015. doi: 10.1016/j.epsl.2015.01.006.

Oi, T. Calculations of reduced partition function ratios of monomeric and dimeric boric acids and borates by the *ab initio* molecular orbital theory. *J. Nucl. Sci. Technol.*, 37(2):166–172, 2000.

Otto, A. H. The gas phase acidity of HBF_4 (HF–BF_3). *Phys. Chem. Comm.*, 2(12):62–66, 1999.

Palaniappan, S. and Devi, S. L. Novel chemically synthesized polyaniline electrodes containing a fluoroboric acid dopant for supercapacitors. *J. Appl. Polym. Sci.*, 107(3):1887–1892, 2008.

Penman, D. E., Hönisch, B., Rasbury, E. T., Hemming, N. G., and Spero, H. J. Boron, carbon, and oxygen isotopic composition of brachiopod shells: Intra-shell variability, controls, and potential as a paleo-pH recorder. *Chem. Geol.*, 340:32–39, 2013. doi: 10.1016/j.chemgeo.2012.11.016.

Rae, J. W. B. Boron Isotopes in Foraminifera: Systematics, Biomineralisation, and CO_2 Reconstruction. In Marschall H. R., Foster G., editor, *Boron Isotopes*, pages 107–143. Springer, 2018.

Rae, J. W. B., Burke, A., Robinson, L. F., Adkins, J. F., Chen, T., Cole, C., Greenop, R., Li, T., Littley, E. F. M., Nita, D. C., Stewart, J. A., and Taylor, B. J. CO_2 storage and release in the deep Southern Ocean on millennial to centennial timescales. *Nature*, 562:569–573, 2018. doi: 10.1038/s41586-018-0614-0.

Rosner, M., Pritzkow, W., Vogl, J., and Voerkelius, S. Development and validation of a method to determine the boron isotopic composition of crop plants. *Anal. Chem.*, 83(7):2562–2568, 2011.

Rustad, J. R., Bylaska, E. J., Jackson, V. E., and Dixon, D. A. Calculation of boron-isotope fractionation between $B(OH)_3$(aq) and $B(OH)_4^-$(aq). *Geochim. Cosmochim Acta*, 74(10):2843–2850, 2010. doi: 10.1016/j.gca.2010.02.032.

Scarpiello, D. A. and Cooper, W. J. Heat of solution of boron trifluoride in water and aqueous hydrofluoric acid. *J. Chem. Engineer. Data*, 9(3):364–365, 1964.

Schauble, E. A. Applying Stable Isotope Fractionation Theory to New Systems. In Johnson, C. M., Beard B. L., and Albarede, F., editor, *Geochemistry of non-traditional stable isotopes, Reviews in Mineralogy and Geochemistry, Vol. 55*, pages 65–111; DOI: 10.2138/gsrmg.55.1.65. Mineralogical Society of America, 2004.

Scott, A. P. and Radom, L. Harmonic vibrational frequencies: An evaluation of Hartree-Fock, Møller-Plesset, quadratic configuration interaction, density functional theory and semiempirical scale factors. *J. Phys. Chem.*, 100:16,502–16,513, 1996.

Urey, H. C. The thermodynamic properties of isotopic substances. *J. Chem. Soc.*, :562–581, 1947.

Vanderryn, J. Infrared Spectrum of BF_3. *J. Chem. Phys.*, 30(1):331–332, 1959. doi: 10.1063/1.1729915.

Wamser, C. A. Hydrolysis of fluoboric acid in aqueous solution. *J. Am. Chem. Soc.*, 70(3):1209–1215, 1948.

Wamser, C. A. Equilibria in the system boron trifluoride–water at 25°C. *J. Am. Chem. Soc.*, 73(1): 409–416, 1951.

Wei, G., Wei, J., Liu, Y., Ke, T., Ren, Z., Ma, J., and Xu, Y. Measurement on high-precision boron isotope of silicate materials by a single column purification method and MC-ICP-MS. *J. Anal. At. Spectrom.*, 28(4):606–612, 2013.

Zeebe, R. E. Stable boron isotope fractionation between dissolved $B(OH)_3$ and $B(OH)_4^-$. *Geochim. Cosmochim. Acta*, 69(11):2753–2766, 2005.

Zeebe, R. E. Kinetic fractionation of carbon and oxygen isotopes during hydration of carbon dioxide. *Geochim. Cosmochim. Acta*, 139:540–552, 2014. doi: 10.1016/j.gca.2014.05.005.